ELSEVIER

Biophysical Chemistry 119 (2006) 170 – 185

Biophysical Chemistry

http://www.elsevier.com/locate/biophyschem

The structure of human apolipoprotein E2, E3 and E4 in solution. 2. Multidomain organization correlates with the stability of apoE structure

Vanessa Clément-Collin [a,1], Anne Barbier [a,b,1], Alexander D. Dergunov [c,*], Athanase Visvikis [b], Gérard Siest [b], Michel Desmadril [d], Masa Takahashi [e], Lawrence P. Aggerbeck [a]

[a] *Centre de Génétique Moléculaire UPR 2167, Centre National de la Recherche Scientifique, Avenue de la Terrasse, 91198 Gif-sur-Yvette, France*
[b] *Centre du Médicament, Université Henri Poincaré Nancy 1, 30 rue Lionnois, 54000 Nancy, France*
[c] *National Research Centre for Preventive Medicine, 10 Petroverigsky Street, 101953 Moscow, Russia*
[d] *Université de Paris XI, Bât. 430, 91405 Orsay, France*
[e] *Institut Curie, University Orsay Paris XI, 91405 Orsay, France*

Received 14 March 2005; received in revised form 2 June 2005; accepted 21 July 2005
Available online 25 August 2005

Abstract

The stabilities toward thermal and chemical denaturation of three recombinant isoforms of human apolipoprotein E (r-apoE2, r-apoE3 and r-apoE4), human plasma apoE3, the recombinant amino-terminal (NT) and the carboxyl-terminal (CT) domains of plasma apoE3 at pH 7 were studied using near and far ultraviolet circular dichroism (UV CD), fluorescence and size-exclusion chromatography. By far UV CD, thermal unfolding was irreversible for the intact apoE isoforms and consisted of a single transition. The r-apoE3 was found to be less stable as compared to the plasma protein and the stability of recombinant isoforms was r-apoE4 < r-apoE3 < r-apoE2. The thermal denaturation of the isolated NT- and CT-domains of apoE3 was largely reversible and included two transitions. The NT-domain was more resistant to heating than the CT-domain, both of which were more resistant than the intact protein. By near UV CD, the thermal unfolding was biphasic. When compared, thermal unfolding of the secondary and tertiary structures appeared to occur concurrently in r-apoE2 whereas heating affected the tertiary structure, initially, in r-apoE3 and r-apoE4. Denaturation with guanidine hydrochloride did not follow a two-state transition. A three-state treatment of the denaturation curves revealed the order of stability as r-apoE4 < r-apoE3 < r-apoE2 for the whole proteins as well as that for the NT-domains, as established by fluorescence and far UV CD spectroscopy, whereas the CT-domains had roughly similar stabilities. There are isoform-specific differences in the stability and in the state of association and the unfolding of both the NT- and CT-domains may be more complex than a two-state transition.

Keywords: Apolipoprotein E; Protein conformation; Domain structure; Secondary and tertiary structure

1. Introduction

Human apolipoprotein E (apoE) contains three major alleles apoE2, apoE3 and apoE4 with single cysteine–arginine interchanges at positions 112 and 158. The structure–function relations that differ drastically for the three isoforms are outlined in the preceding paper [1] where the tertiary and quaternary structure of three recombinant isoforms was studied. The protein is composed of an N-terminal (NT, residues 1–191) domain that bears low-density lipoprotein (LDL) receptor-binding domain sites, and a C-terminal (CT, residues 210–299) domain which contains lipoprotein binding and apoE self-association sites. The NT-domain is comprised of a four-helix bundle [2], while the structural organization of the CT-domain is not precisely known. The apoE domain

Abbreviations: apoE, apolipoprotein E; apo, apolipoprotein; CD, circular dichroism; CT, carboxyl-terminal; DTT, dithiothreitol; GuHCl, guanidine hydrochloride; N, native state of the protein; NT, amino-terminal; p, plasma; r, recombinant; R_s, Stokes radius; U, unfolded state of the protein; UV, Ultraviolet; V_e, elution volume.

* Corresponding author. Tel.: +7 95 927 0324; fax: +7 95 928 5063.
E-mail address: dergunov@img.ras.ru (A.D. Dergunov).

[1] Both authors contributed equally to the study.

0301-4622/$ - see front matter © 2005 Elsevier B.V. All rights reserved.
doi:10.1016/j.bpc.2005.07.009

structure contributes to apolipoprotein self-association [3–5] and significantly changes when the whole apolipoprotein molecule [6,7] or its receptor-binding fragment [8–14] binds to lipids. However, far less knowledge is available about the subtle differences in the structural organization of three apoE isoforms. Intra-domain structure may discriminate isoforms in terms of: (i) receptor binding [15]; (ii) apoE self-association [16]; (iii) efficient CT-domain mediated binding of apoE2 and apoE3 but not of apoE4 to β-amyloid peptide [17]; and (iv) interaction of apoE with the lipids. Interactions with lipids are characterized by a preferential accumulation of apoE4 in very low-density lipoproteins and apoE3 in high density lipoproteins [18,19], by different conformations of the lipid-bound isoforms [6,20,21] and by different kinetics upon interaction with lipid [22]. Interaction between the NT- and CT-domains is suggested by the existence of Arg61–Glu255 salt bridge in apoE4 [19] and by the inhibition of apoE2 binding to the LDL receptor by part of the CT-domain [23]. The model of two independent and non-interacting domains [24,25] for isoforms other than apoE3 needs more detailed examination.

The existence of more than one structure at the transition from the native to the unfolded state seems to be a common feature of exchangeable apolipoproteins such as apoA-I [26–28], apoA-II [29] and apoC-I [30]. Initially, two sequential two-state transitions in CT- and NT-domains were deduced from the guanidine hydrochloride (GuHCl) denaturation curve of plasma apoE3 [25]; the presence of a partially folded intermediate in the NT-domain was described later, more prominent in apoE4 as compared to apoE3, apoE2 unfolded by a two-state mechanism [24,31,32]. However, if the possibility of a domain interaction was initially not considered [24,25], an interaction with the CT-domain that appeared to destabilize the NT-domain in apoE2 and apoE3, but less so for apoE4, was suggested later [22,31]. These authors gave no evidence for any intermediate structure(s) at the unfolding of the CT-domain; however, Choy at al. [33] suggested that the native tetrameric CT-domain dissociated firstly to coiled–coiled dimer rather than to monomer upon GuHCl-induced denaturation. Moreover, a two-domain structure in the 267–289 region of the CT-domain was revealed by circular dichroism and ^{1}H NMR [34]. The additional stabilization of the apolipoprotein upon self-association [4,31] might contribute to a multi-state transition.

In the present study we provide new information on the structure of three recombinant apoE isoforms by comparing their stability to temperature- and GuHCl-induced denaturation. We report first, a differential stability to unfolding, apoE4 < apoE3 < apoE2, as assessed by temperature and GuHCl and, second, a complex, non-two-state transition within CT- and NT-domains during chemical unfolding that is closely connected to the different association states of these isoforms.

2. Materials and methods

2.1. Isolation of proteins

Three recombinant human apoE isoforms, r-apoE2, r-apoE3 and r-apoE4, were produced by heterologous expression in *E. coli* [35,36]. The purity of the proteins was evaluated by SDS-PAGE and mass spectrometry. Prior to use, the proteins were denatured for 24 h at 20 °C in 6 M GuHCl, 100 mM Tris–HCl, pH 7.8, 1 mM EDTA and 2% β-mercaptoethanol and then dialyzed extensively at 4 °C against 100 mM NH_4HCO_3, 1 mM DTT, and finally against 20 mM sodium phosphate buffer pH 7.4, 1 mM DTT for the circular dichroism and fluorescence experiments. The amino-terminal domain of human apoE3 (r-NT-domain) was expressed in *E. coli* BL 21 DE3 cells transformed with the pet11a vector from Novagen containing the cDNA sequence of the apoE3 NT-domain inserted between the BamH1 (5′) and Nde1 (3′) sites of the polylinker. Expression of the protein was obtained by induction of the T7 promoter with 0.4 mM IPTG for 2 h once the culture attained an optical density of 0.3 units at 600 nm. Recombinant protein was purified as previously described [37]. Human plasma apoE3 (p-apoE3) and the carboxyl-terminal domain of plasma apoE3 (p-CT-domain) were prepared as described previously [38].

For the temperature denaturation experiments, protein concentrations were determined by tryptophan fluorescence [39] or by measuring the absorbance at 280 nm in the presence of 6 M GuHCl, 2% β-mercaptoethanol using an extinction coefficient of 1.32 ml/mg cm^{-1} [40]. Samples for the equilibrium unfolding by GuHCl were prepared in the presence of increasing amounts of GuHCl and incubated at 20 °C for at least 15 h. Solutions were degassed before use. The GuHCl concentration was determined by measuring the refractive index of the solution, protein concentrations were determined by measuring the optical density at 280 nm in the presence of 3 M GuHCl [40].

2.2. Near and far ultraviolet circular dichroism (UV CD) measurements

For the temperature denaturation studies, near UV CD spectra were measured with a Jasco J700 spectropolarimeter in a 1 cm quartz cuvette on 200 µl of sample with a protein concentration between 0.5 and 1 mg/ml in 20mM sodium phosphate, pH 7, 1 mM DTT. Spectra were recorded on the same sample between 250 and 330 nm at 6–8 constant temperatures, between 15 and 80 °C, using a 100 nm/min scan speed, a 0.5 s response, a 0.2 nm resolution and a 2 nm bandwidth. Each spectrum was the average of 8 accumulations. The ellipticity at 292 nm was also measured continuously from 15 to 80 °C and then from 80 back to 15 °C, using a scan rate of 1 °C/min, a 2 nm bandwidth, a 0.2 °C resolution, and a 16 s response time. Far UV CD spectra were measured on samples having a protein

concentration of approximately 0.1 mg/ml using a 0.1 cm quartz cuvette. Spectra between 185 and 300 nm were recorded at temperatures between 15 and 80 °C, using the same parameters as for the near UV spectra. The ellipticity at 222 nm was also measured continuously between 15 and 80 °C and then from 80 back to 15 °C using the same parameters as for the near UV spectra. The ellipticity was normalized (θ_N^{λ}) using the following relationships:

$$\theta_N^{222\,nm} = \frac{\theta_T^{222\,nm} - \theta_{15\,°C}^{222\,nm}}{\theta_{15\,°C}^{222\,nm} - \theta_{80\,°C}^{222\,nm}} \quad (1)$$

$$\theta_N^{292\,nm} = \frac{\theta_T^{292\,nm} - \theta_{min}^{292\,nm}}{\theta_{max}^{292\,nm} - \theta_{min}^{292\,nm}} \quad (2)$$

where θ_T^{λ} is the ellipticity at temperature T, and wavelength λ, θ_{max}^{λ} and θ_{min}^{λ} are the maximum and minimum ellipticities, respectively, at wavelength λ.

In the GuHCl denaturation study, far UV CD spectra were recorded in a 2 mm path length quartz cell on a Jobin–Yvon Mark V Spectropolarimeter (Jobin–Yvon, Longjumeau, France) piloted by a micro computer and calibrated with a solution of 0.1% D-10-camphorsulfonic acid. Spectra were measured at 20 °C at 0.115 mg/ml for r-apoE2 and r-apoE4 and 0.056 mg/ml for r-apoE3. Spectra are the average of three scans recorded between 215 and 250 nm, with a time resolution of 1 s, a 2 nm bandwidth and at 60 nm/min. In the absence of GuHCl, the spectra were recorded between 200 and 250 nm. Protein spectra were corrected by subtracting spectra obtained in absence of protein. The molar ellipticity [θ] at each wavelength was calculated from the relationship:

$$[\theta] = \frac{\theta_\lambda \cdot \mathrm{MRW}}{10 \cdot l \cdot c} \quad (3)$$

where MRW is the mean residue weight, θ_λ is the measured ellipticity (in degrees) at wavelength λ, l is the cuvette path length (in cm), and c is the protein concentration (in g/ml). A mean residue weight of 113.5 was used for the r-apoE isoforms. The fraction of α helix, f_H, in the proteins was estimated from the molar ellipticity at 222 nm, θ_{222}, according to Chen et al. [41] using Eq. (4):

$$[\theta]_{222} = -30300 f_H - 2340. \quad (4)$$

2.3. Fluorescence measurements

Fluorescence emission spectra were obtained using the same samples of recombinant apoE isoforms that were used for circular dichroism GuHCl denaturation studies. Spectra were measured at 21 °C with a Perkin-Elmer 650-40 (Palo Alto, CA.) fluorescence spectrometer between 300 and 400 nm at 60 nm/min with excitation at 295 nm. Protein spectra were corrected by subtracting spectra obtained in the absence of protein. The wavelength of the maximum of the fluorescence emission intensity was determined by peak fitting. The average emission wavelength <λ>, was also calculated using the equation:

$$\langle\lambda\rangle = \frac{\sum_{i=\lambda_1}^{\lambda_N} (F_i \cdot \lambda_i)}{\sum_{i=\lambda_1}^{\lambda_N} F_i} \quad (5)$$

where F is the fluorescence intensity and λ the wavelength. The average wavelength takes into account both changes in the shape and position of the spectrum and is less subject to error than measurements at a single wavelength [42].

2.4. Size-exclusion chromatography

Size-exclusion chromatography of the r-apoE isoforms was performed at 4 °C at a flow rate of 0.5 ml/min using a Superose 12 column (1 × 30 cm) equilibrated with 100 mM NH_4HCO_3, 1 mM β-mercaptoethanol and various concentrations of GuHCl (0 to 4 M). Approximately 20 μg of protein in 100 mM NH_4HCO_3 was injected onto the column, and the elution profile was determined by monitoring the optical density at 280 nm. The column was calibrated with proteins of known molecular weight and Stokes radii (R_s) as determined by sedimentation and diffusion data [43,44]. Stokes radii of the native and unfolded r-apoE isoforms were determined as described by Uversky [44].

Three components (monomer, dimer and tetramer) were observed in solutions of r-apoE isoforms. The mean elution volume, <V_e>, can be defined by the relationship Eq. (6):

$$\langle V_e\rangle = f_T \cdot V_{eT} + f_D \cdot V_{eD} + f_M \cdot V_{eM} \quad (6)$$

where f_T, f_D, f_M are the fractions of tetramer, dimer and monomer, respectively, and V_{eT}, V_{eD}, V_{eM} are the elution volumes of the tetramer, dimer and monomer, respectively. The relative populations of each of the components were determined by fitting a series of Gaussian curves to the chromatograms. The change in the elution profile was investigated, as a function of the concentration of GuHCl, by following the change in the partition coefficient, K_D, determined from the relationship Eq. (7):

$$K_D = \frac{V_e - V_o}{V_t - V_o} \quad (7)$$

where V_e is the elution volume of the protein, V_t is the total included volume of the column (the V_e of $NaNO_3$ or β-mercaptoethanol) and V_o is the exclusion volume of the column (the V_e of Blue Dextran).

2.5. Treatment of the denaturation data

In order to compare the GuHCl denaturation process as assessed by the different techniques, the experimental

results were transformed into the fraction of native molecules (f_N) calculated according to Eq. (8):

$$f_N = \frac{X - X_D}{X_N - X_D} \quad (8)$$

where X is the measured parameter (V_e, $[\theta]$ or λ_{max}) at a given GuHCl concentration, X_D is the value of the parameter for the protein in the totally unfolded state, X_N is the value of the parameter for the protein in the native (folded) state. Apparent free energies of denaturation ΔG_D^{H2O} were estimated for each of the transitions of the denaturation curves using a three-state transition model [45–47] assuming the following scheme:

$$N \underset{K_{app}}{\overset{K_{n,i}}{\rightleftharpoons}} I \overset{K_{i,u}}{\rightleftharpoons} U \quad (9)$$

where N, I and U are the folded, intermediate and unfolded states, respectively. $K_{n,i}$, $K_{i,u}$ are the equilibrium constants for the transition between the folded state and the intermediate state and between the intermediate state and the unfolded state, respectively, and K_{app} is the apparent equilibrium constant between the native state and the unfolded state. The following parameters were used, y_n, y_u, y_i, which correspond to the experimental values obtained for the protein in the folded state, in the fully unfolded state and in the intermediate state, respectively. The fractional change in the optical parameter being followed in the transition from N to U is $\alpha_i=(y_i-y_n)/(y_u-y_n)$ and the observed fraction of unfolded material f_{obs} may be expressed:

$$f_{obs} = \alpha_i \cdot f_i + f_u \quad (10)$$

where f_i and f_u are the fractions of the intermediate and the unfolded species, respectively. K_{app} may be expressed in terms of the observed fraction of unfolded material f_{obs} as follows:

$$K_{app} = \frac{f_{obs}}{1 - f_{obs}}. \quad (11)$$

Using the sum of the three species, $f_n+f_i+f_u=1$, and the definitions of the constants, $K_{n,i}=f_i/f_n$ and $K_{i,u}=f_u/f_i$ in Eqs. (10) and (11) leads to the following expression:

$$f_{obs} = \frac{\alpha_i \cdot K_{n,i} + K_{n,i} \cdot K_{i,u}}{1 + K_{n,i} + K_{n,i} \cdot K_{i,u}}. \quad (12)$$

The constants $K_{n,i}$ and $K_{i,u}$ may also be defined, according to Tanford [45] as:

$$K = K^{H_2O} \cdot (1 + k \cdot a)^{\Delta n} \quad (13)$$

where K is the apparent equilibrium constant at a particular concentration of GuHCl, K^{H2O} is the equilibrium constant in the absence of GuHCl, k is the binding constant of the denaturant agent (0.8 when a is expressed in GuHCl molarity), a is the GuHCl molarity and Δn is the variation in the number of binding sites of GuHCl

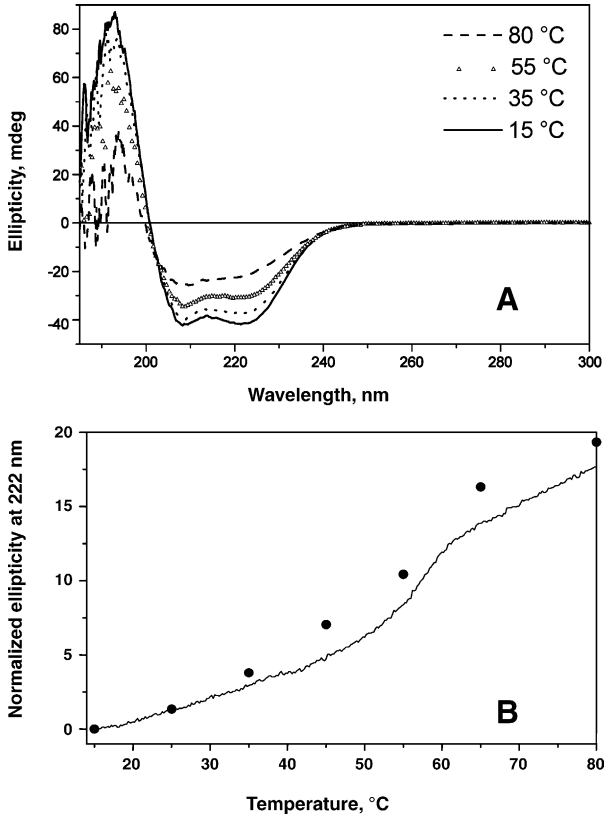

Fig. 1. Far ultraviolet circular dichroism analysis of the temperature-induced unfolding of human plasma apoE3. (A) Far UV CD spectra of p-apoE3 (0.1 mg/ml in 20 mM sodium phosphate pH 7, 1 mM DTT) were recorded at the temperatures indicated. (B) The ellipticity at 222 nm of p-apoE3 was recorded at intervals (closed circles) and continuously as a function of the temperature (solid line). The values of the ellipticity were normalized by subtraction of the ellipticity measured at 15 °C.

Table 1
Far and near UV CD parameters for the temperature-induced denaturation of apoE isoforms and apolipoprotein domains

Spectroscopy		T_m(app) °C	ΔH(app), kcal/mol	ΔS(app), kcal/mol/K
Far UV CD	r-apoE2	58.7±0.06	70.1±1.70	0.21±0.005
	r-apoE3	49.6±0.058	40.2±0.83	0.12±0.0025
	p-apoE3	55.9±0.16	65.0±3.89	0.19±0.012
	r-apoE4	47.3±0.06	33.8±0.73	0.10±0.0023
	p-CT	60.6±0.07	52.5±0.0028	0.15±0.925
	r-NT	65.5±0.16	61.5±1.76	0.18±0.005
Near UV CD	r-apoE2	61.6±0.35	57.3±5.37	0.17±0.016
	r-apoE3	39.3±0.2	48.9±3	0.15±0.01
	p-apoE3	56.6±0.68	39.9±8.52	0.12±0.025
	r-apoE4	39.1±0.17	61.6±4.14	0.19±0.013

Due to only partial reversibility of the transitions, the melting temperature and Van't Hoff enthalpy determined by a conventional Van't Hoff analysis should be considered as apparent T_m(app) and ΔH(app) values. In such an analysis, the baselines for the folded and unfolded states, were fixed as ellipticity values at 15 and 80 °C, respectively, in far UV CD (Eq. (1)) and as maximal and minimal ellipticity values in near UV CD (Eq. (2)) due to small pre- and posttransitional regions of the thermal unfolding curves. The upper limit of the uncertainties due to different baseline interpolation, if any, may not exceed 0.5 °C (2 °C for near UV CD) and 3 kcal/mol for the T_m(app) and ΔH(app), respectively.

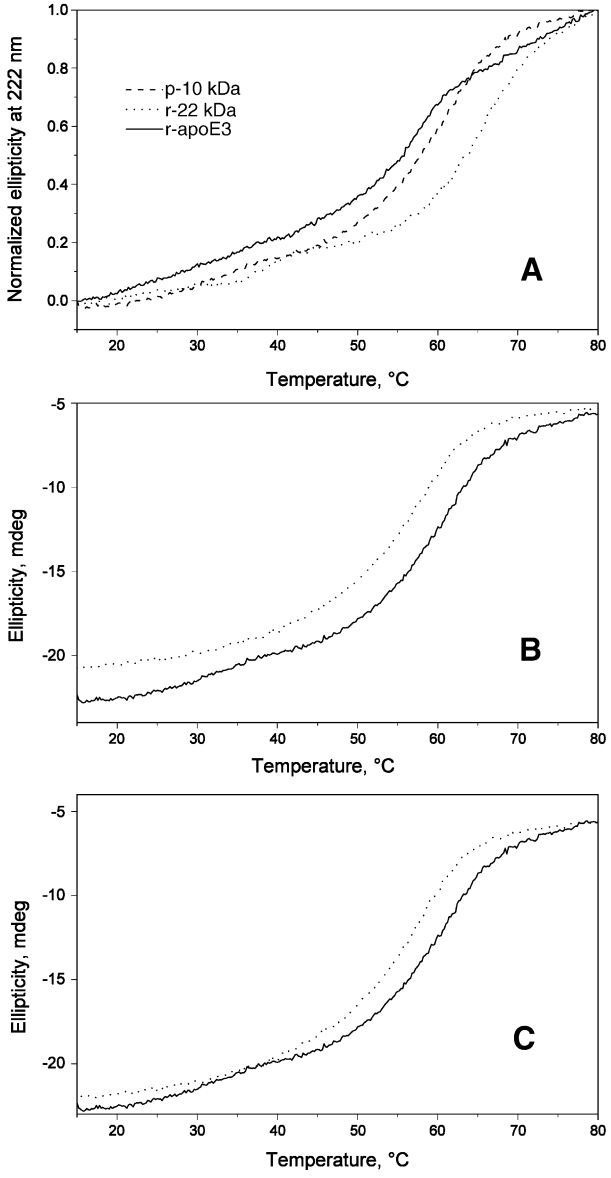

Fig. 2. Temperature-induced denaturation of plasma apoE3, the recombinant amino-terminal domain and the plasma carboxyl-terminal domain. (A), the ellipticity at 222 nm was measured continuously while increasing the temperature from 15 to 80 °C (scan rate 1 °C per min) at a protein concentration of about 0.1 mg/ml in 20 mM sodium phosphate pH 7, 1 mM DTT. The data was normalized to permit comparison of the denaturation curves directly. (B), the reversibility of the denaturation curve for r-NT-domain; (C), the reversibility of the denaturation curve for p-CT-domain. The ellipticity at 222 nm was measured continuously while increasing the temperature from 15 to 80 °C (scan rate 1 °C per min, solid line) and then decreasing temperature to 15 °C (scan rate 1 °C per min, dotted line).

between the two states. Combining Eqs. (12) and (13) and using $K_{n,i}^{H2O} \cdot K_{i,u}^{H2O} = K_{n,u}^{H2O}$ lead to:

$$f_{obs} = \frac{\alpha_i \cdot K_{n,i}^{H_2O} \cdot (1 + k \cdot a)^{\Delta n_{n,i}} + K_{n,u}^{H_2O} \cdot (1 + k \cdot a)^{\Delta n_{n,u}}}{1 + K_{n,i}^{H_2O} \cdot (1 + k \cdot a)^{\Delta n_{n,i}} + K_{n,u}^{H_2O} \cdot (1 + k \cdot a)^{\Delta n_{n,u}}}. \quad (14)$$

Denaturation curves for each recombinant apoE isoform were fitted according to Eq. (14) by plotting f_{obs} as a function of $k \cdot a$. Five parameters were varied: $K_{n,u}^{H2O}$, $K_{n,i}^{H2O}$, Δn_{nu}, Δn_{ni} and α_i. From the best fit of the data, the fraction of each species as a function of the concentration of GuHCl was calculated. The apparent free energy of denaturation without GuHCl was calculated using the following relationship:

$$\Delta G_{n,u}^{H_2O} = -RT \ln K_{n,u}^{H_2O} \quad (15)$$

$$\Delta G_{n,i}^{H_2O} = -RT \ln K_{n,i}^{H_2O} \quad (16)$$

$$\Delta G_{i,u}^{H_2O} = \Delta G_{n,u}^{H_2O} - \Delta G_{n,i}^{H_2O}. \quad (17)$$

3. Results

3.1. Temperature denaturation study

3.1.1. Far UV CD

The effect of temperature upon the optical activity of proteins was assessed in two ways. The ellipticity was measured between 185 and 300 nm at eight temperatures between 15

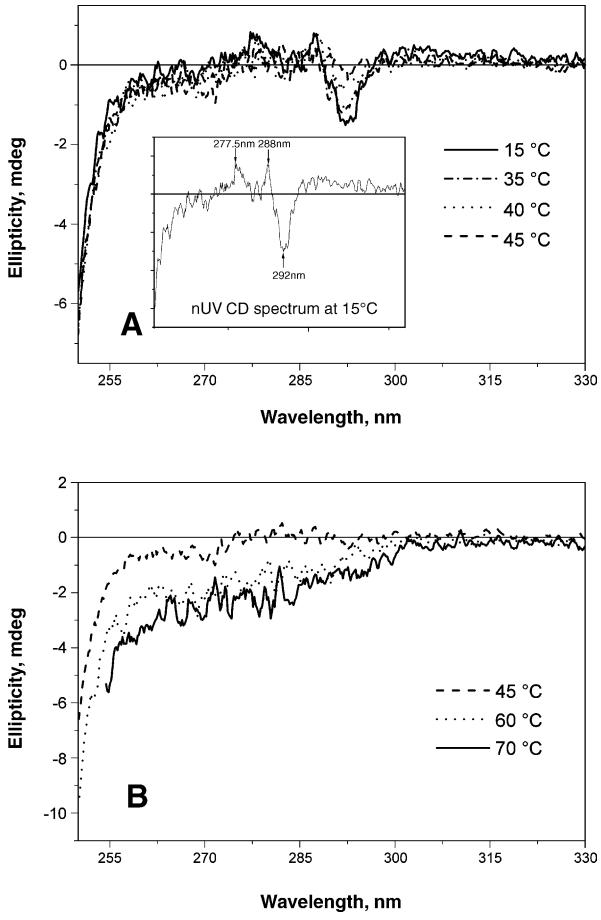

Fig. 3. Near ultraviolet circular dichroism spectra of recombinant apoE3 recorded at different temperatures. The ellipticity between 250 and 330 nm of the protein at 1 mg/ml in 20 mM sodium phosphate pH 7, 1 mM DTT was recorded at several temperatures. (A) 15–35–40–45 °C, (B) 45–60–70 °C. The inset shows the spectrum of r-apoE3 at 15 °C.

and 80 °C. In an independent experiment, the ellipticity at a single wavelength, 222 nm, was measured continuously as the temperature was increased from 15 to 80 °C.

The far UV CD spectrum of p-apoE3 measured at 15 °C displays two minima at 208 and 222 nm, and is typical of a protein with a highly helical structure (Fig. 1A). With increasing temperatures the optical activity decreases indicating a loss of helicity (Fig. 1A,B). The values of the ellipticity at 222 nm determined from the spectra at selected temperatures follow closely the values measured while continuously increasing the temperature from 15 to 80 °C (Fig. 1B), suggesting that the rate of increase in the temperature during the continuous scan is slow enough for the sample to equilibrate. A single transition was observed between 15 and 80 °C. At 80 °C, the far UV CD curves of p-apoE3 (Fig. 1A), r-apoE3, the r-NT-domain of apoE3 and the p-CT-domain (results not shown), still exhibit minima in their spectra at 208 and 222 nm suggesting that some α-helical structure remains at this temperature.

We measured continuously, from 15 to 80 °C, the ellipticities at 222 nm for p-apoE3, r-apoE2, r-apoE3, r-apoE4, r-NT-domain and p-CT-domain. The calculated α-helical content at 15 °C ranged from 51% (r-apoE4) to 64% (r-apoE2 and r-apoE3). The normalized temperature scans show a loss of optical activity with increasing temperature that occurs at the lowest temperatures for r-apoE4 followed by r-apoE3, p-apoE3 and then r-apoE2. The thermal denaturation scans of p-apoE3, r-apoE3 and r-apoE4 exhibit one major transition which occurs between 40 and 60 °C. A second minor transition between 20 and 40 °C is readily apparent in the case of r-apoE2. The apparent mid-transition temperatures and Van't Hoff enthalpies were estimated for the major transitions, assuming a two-state transition (Table 1). Both the higher mid-transition temperature and the Van't Hoff enthalpy of r-apoE2 suggest that it is the most stable to thermal denaturation of the three recombinant isoforms, whereas r-apoE4 is the least stable. Recombinant apoE3 has a lower mid-transition temperature and a lower Van't Hoff enthalpy than plasma apoE3, suggesting that the secondary structure of r-apoE3 is less stable to thermal denaturation than that of p-apoE3. The effect of temperature upon the secondary structure of the NT- and CT-domains of apoE3 as compared to the intact protein was also evaluated. The

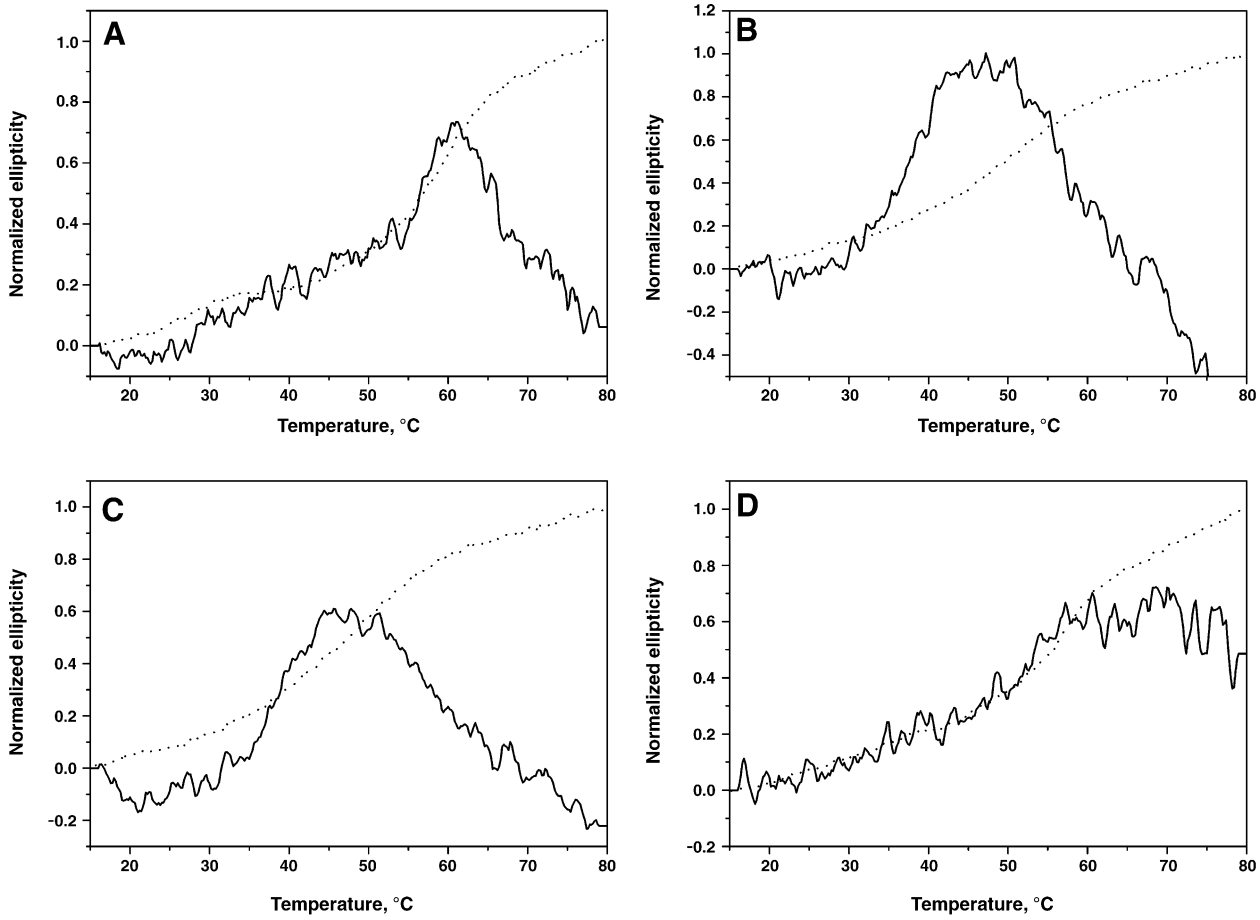

Fig. 4. Near UV and far UV CD denaturation curves of recombinant and plasma apoE. (A), r-apoE2; (B), r-apoE3; (C), r-apoE4; and (D), p-apoE3. The thermal unfolding curves obtained by far UV CD (normalized ellipticity at 222 nm, dots) and near UV CD (normalized ellipticity at 292 nm, solid line) are plotted.

normalized temperature scans of the ellipticity at 222 nm (Fig. 2A), the mid-transition temperatures and the Van't Hoff enthalpies (Table 1) show that the amino-terminal domain is more stable to thermal denaturation, than the carboxyl-terminal domain. The intact plasma protein exhibits a higher Van't Hoff enthalpy and a lower mid-transition temperature than the NT- and the CT-domains individually. Further, both domains display two transitions in the 20–45 °C and the 50–80 °C range (Fig. 2B). However, the first transition is much less apparent for the intact protein which appears to have only one major transition in the 50–80 °C range. For all the proteins, heating from 15 to 80 °C results in a loss of roughly 50% of the CD signal, except for the CT-domain for which 75% of the CD signal is lost.

The reversibility of the effects of heating upon the secondary structure of p-apoE3, r-apoE2, r-apoE3, r-apoE4, r-NT-domain and p-CT-domain was evaluated. The percents of the initial ellipticities at 222 nm recovered after first increasing the temperature from 15 to 80 °C and then decreasing the temperature to 15 °C were 80–85% for each domain while there was no recovery of the secondary structure for intact protein, recombinant or plasma. Upon cooling after heating, the denaturation curves of the NT- and CT-domains display a hysteresis suggesting the slower folding rate and/or some irreversible change of apolipoprotein structure at elevated temperatures as observed for apoA-I [27] and apoC-I [30]. However, since irreversible changes are relatively slow compared to the protein heat unfolding, they do not preclude equilibrium thermodynamic analysis of the unfolding transition. After renaturation, the far UV CD spectra of the NT- and CT-domains remain characteristic of helical proteins and are similar to the initial spectra measured at 15 °C. In contrast, the spectrum of plasma apoE3 obtained at 15 °C, following thermal denaturation at 80 °C, is intermediate between the spectrum at 80 °C and the initial spectrum at 15 °C.

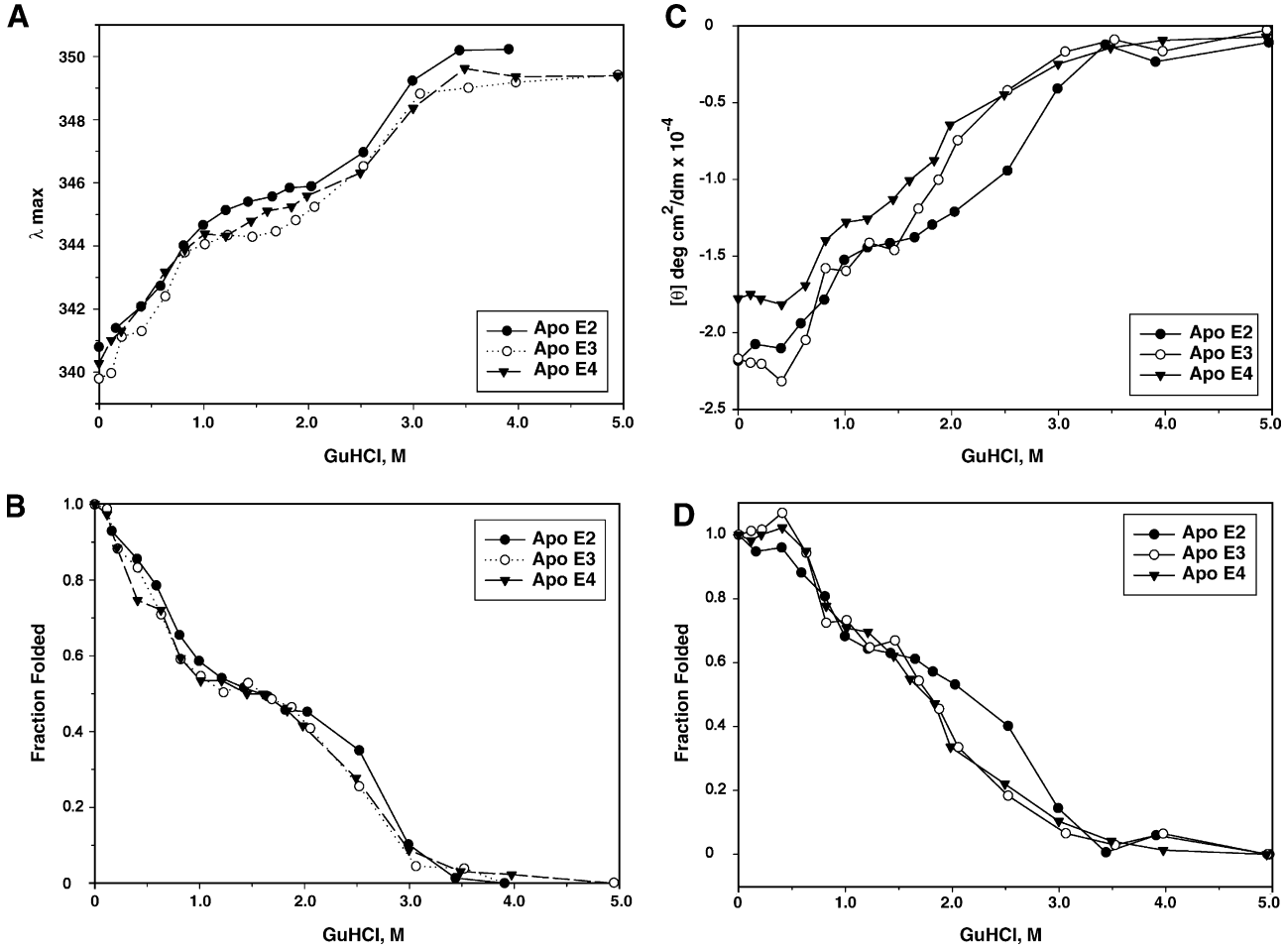

Fig. 5. Fluorescence and CD spectroscopic analysis of the guanidine hydrochloride induced denaturation of recombinant apoE isoforms. (A) The wavelength of the maximum of fluorescence intensity is plotted as a function of the GuHCl concentration. (B) The fraction of native structure is plotted as a function of the denaturant concentration. Samples containing 0.115 mg/ml for r-apoE2 and r-apoE4 and 0.056 mg/ml for r-apoE3 were excited at 295 nm and spectra were recorded at 21 °C. (C) The molar ellipticity at 222 nm is plotted as a function of the concentration of GuHCl. (D) The fraction of native structure is plotted as a function of the denaturant concentration. Spectra of solutions containing 0.115 mg/ml for r-apoE2 and r-apoE4 and 0.056 mg/ml for r-apoE3 were recorded at 20 °C using a 2 mm cell.

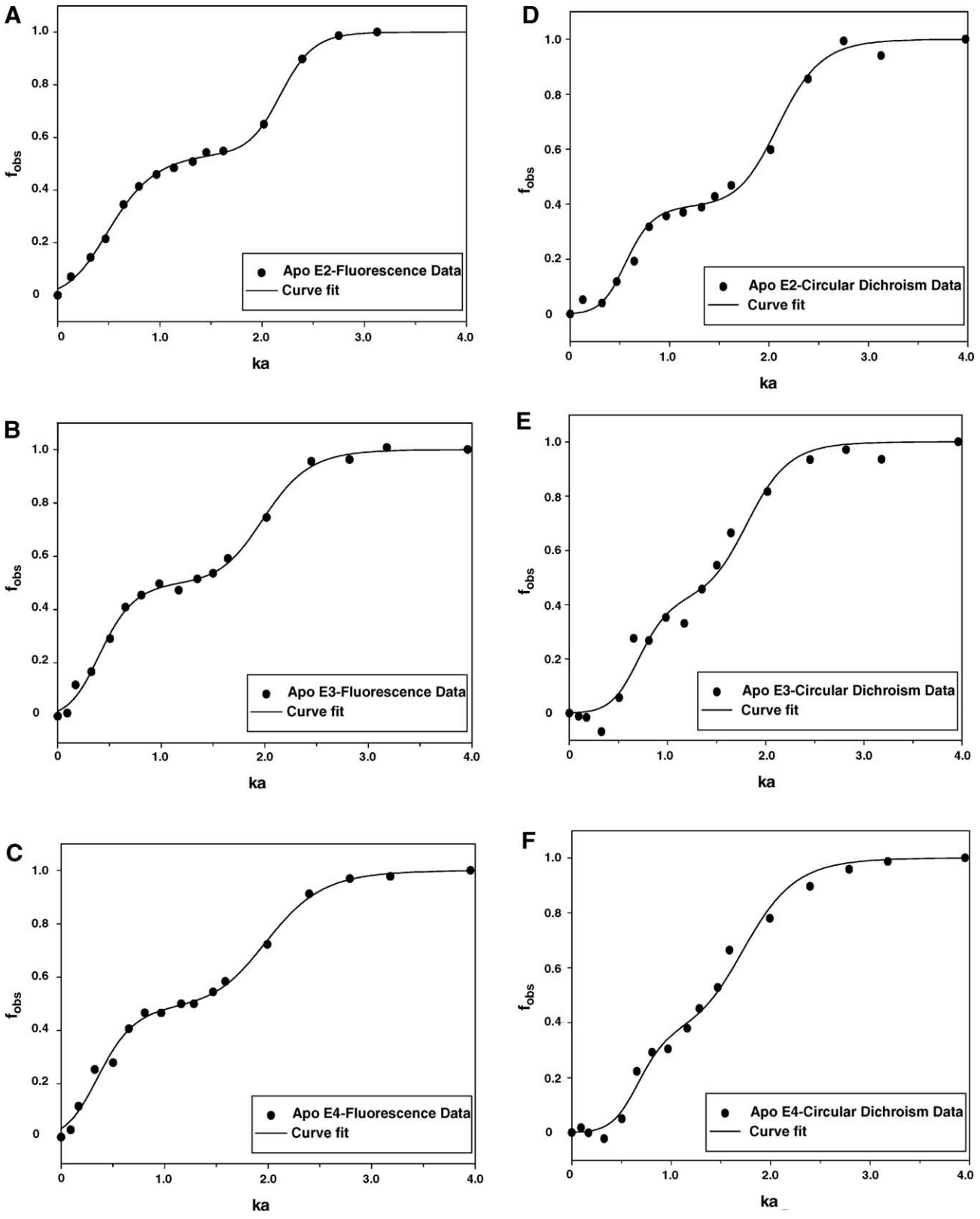

Fig. 6. Three-state transition analysis of the fluorescence (A–C) and CD (D–F) data for the GuHCl denaturation of recombinant apoE isoforms. The best fits (solid lines) of the experimental data (points) are shown. (A,D), r-apoE2; (B,E), r-apoE3; (C,F), r-apoE4.

3.1.2. Near UV CD

In order to evaluate the tertiary structural changes that occur upon heating, near UV CD spectra (250–330 nm) of r-apoE3 were recorded at selected temperatures between 15 and 80 °C (Fig. 3). At 15 °C, the near UV CD spectrum of r-apoE3 shows, as do those of r-apoE2, p-apoE3, r-apoE4 and r-NT-domain (results not shown), a minimum at about 292 nm, and two maxima at about 277 and 288 nm. Increasing the temperature eliminates gradually the minimum and the two maxima. The optical activity at 292 nm first decreases with increasing temperatures between 15 and 45 °C and then increases between 45 and 70 °C, probably, due to the protein aggregation. We measured continuously the ellipticity at 292 nm for the r-apoE2, r-apoE3, r-apoE4, and p-apoE3 from 15 to 80 °C. The effect of temperature upon the three recombinant isoforms is similar consisting first of a loss of optical activity followed by increasing negative optical activity. The minimum in the optical activity occurs at about 45 °C for r-apoE3 and r-apoE4 whereas for r-apoE2 it occurs at about 62 °C. The comparison of the T_m(app) values (Table 1) shows the order of resistance of the tertiary structure to thermal denaturation: r-apoE4 < r-apoE3 < p-apoE3 < r-apoE2, identical to that established by the far UV CD study (Table 1). Following denaturation no signal was recovered, in the near UV CD region, after decreasing the temperature from 80 to 15 °C for r-apoE2 and p-apoE3 (results not shown). The tertiary thermal unfolding appears to be irreversible.

The changes of the secondary and tertiary structures resulting from heating were compared by plotting together the normalized near and far UV CD denaturation curves (Fig. 4). The near UV CD transition occurs at lower temperatures than the far UV CD transition for r-apoE3 and r-apoE4 (Table 1), whereas the two transitions seem to occur at the same temperatures for p-apoE3 and r-apoE2 (considering only the second major transition in the far UV for r-apoE2).

3.2. GuHCl denaturation study

3.2.1. Fluorescence spectroscopy

The wavelength of the emission maximum was determined as a function of the GuHCl concentration, although similar results were obtained with the average emission wavelength. The fraction of the protein remaining folded was expressed as a function of the concentration of denaturant (Fig. 5). Two transitions were clearly apparent for each of the recombinant isoforms as has been described for plasma apoE3 [25]. The first transition, between 0 and 1.5 M GuHCl, corresponds to the denaturation of the carboxyl-terminal domain and the second transition, between 1 and 5 M GuHCl corresponds to the unfolding of the amino-terminal domain. The folding of each domain has been shown to be independent from the other [25].

We used a three-state model of denaturation (Eq. (14)) to calculate the apparent free energies of denaturation for each of the transitions (Eqs. (15)–(17)). $\Delta G^{H2O}_{n,u}$, $\Delta G^{H2O}_{n,i}$ and $\Delta G^{H2O}_{i,u}$ correspond to the apparent free energies of denaturation of the intact protein, of the CT- and of the NT-domains, respectively. The experimental and fit data are shown in Fig. 6 and the resulting parameters are presented in Table 2. There are distinct differences in the overall stabilities of the intact proteins as well as in the stabilities of the domains among the isoforms. The overall stability of the r-apoE2 as well as of its NT-domain were markedly greater than that of the other two isoforms and their corresponding NT-domains. The greater stability overall of apoE2 is due to the greater stability of its amino-terminal domain. The CT-domains are clearly less stable than the NT-domains. In contrast, the overall stability as well as the stabilities of each domain individually were the lowest for the r-apoE4.

3.2.2. Far UV CD

The plot of the molar ellipticity at 222 nm versus the GuHCl concentration presented two transitions for each of the isoforms as was the case in fluorescence (Fig. 5). The experimental data were fitted to a three-state model of denaturation (Fig. 6) and the resulting parameters are listed in Table 2. As was the case for the denaturation as followed by fluorescence, the r-apoE4 exhibited the lowest overall stability and the lowest stability for the NT-domain whereas r-apoE2 was the most stable. However, the CT-domain of r-apoE2 appears to be slightly less stable than those of r-apoE3 and r-apoE4. These differences are small (10–20%) however, as compared to the differences in the overall stabilities (21–42%) or to the differ-

Table 2
Fluorescence and far UV CD parameters for the GuHCl-induced denaturation of apoE isoforms

Spectroscopy	Isoform	$K_{n,i}$	$\Delta G_{n,i}$, kcal/mol	$\Delta n_{n,i}$	$K_{i,u}$	$\Delta G_{i,u}$, kcal/mol	$\Delta n_{i,u}$	$K_{n,u}$	$\Delta G_{n,u}$, kcal/mol	$\Delta n_{n,u}$	α
Fluorescence	r-apoE2	0.0481	1.8	7.0	6.72^{-11}	13.6	20.2	3.23^{-12}	15.4	27.2	0.55
	r-apoE3	0.0403	1.9	8.9	2.29^{-7}	8.9	13.9	9.22^{-9}	10.8	22.8	0.51
	r-apoE4	0.0681	1.6	8.2	3.25^{-6}	7.4	11.4	2.21^{-7}	8.9	19.6	0.38
CD	r-apoE2	0.00448	3.2	11.9	5.20^{-8}	9.8	14.8	2.33^{-10}	12.9	26.7	0.40
	r-apoE3	0.00206	3.6	11.2	5.74^{-7}	8.4	13.9	1.18^{-9}	12.0	25.1	0.43
	r-apoE4	0.0022	3.6	11.7	1.17^{-5}	6.6	11.2	2.58^{-8}	10.2	22.9	0.38

The observed transition curves were fitted to a three-state model.

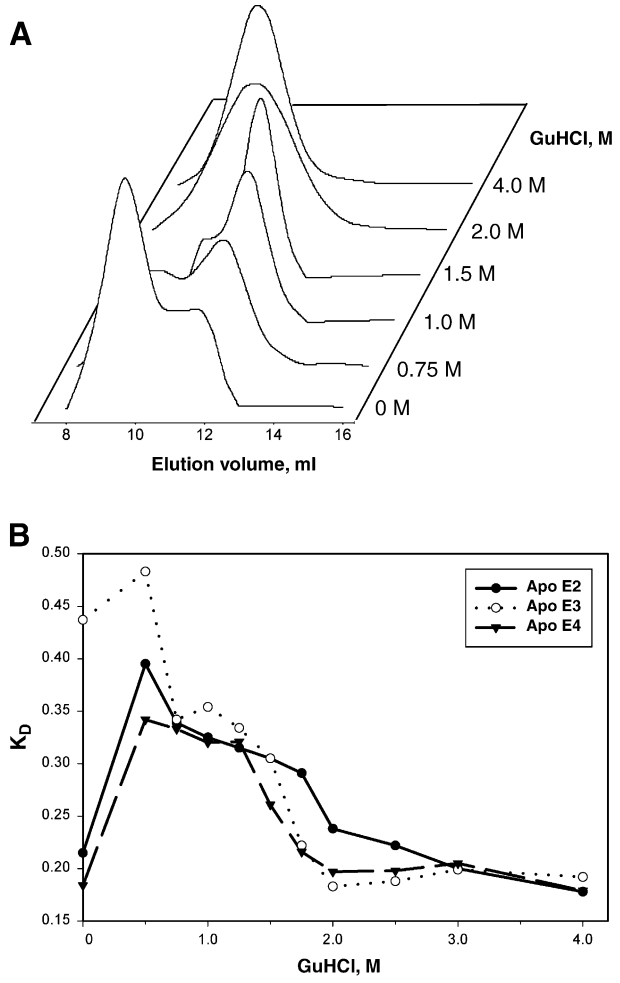

Fig. 7. Size-exclusion chromatography analysis of the guanidine hydrochloride induced denaturation of recombinant apoE isoforms. (A) The elution profiles of the r-apoE2 are shown for GuHCl concentrations between 0 and 4 M. The apoE concentration was 1 mg/ml in 100 mM ammonium bicarbonate, 1 mM β-mercaptoethanol. (B) The coefficients of partition K_D of the three recombinant apoE isoforms with increasing GuHCl concentrations between 0 and 4 M.

ences in the stabilities of the NT-domains (30–45%) of the isoforms.

3.2.3. Size-exclusion chromatography

The permeation properties of the Superose 12 column are practically independent of solvent, temperature, pH and denaturant concentrations [44]. We determined that proteins of known Stokes radii R_s injected onto the Superose 12 column obeyed the equation $1000/V_e = 0.615 \cdot R_s + 58.66$. This equation allows the determination of the apparent R_s values at any concentration of GuHCl. Fig. 7A shows the elution profiles of r-apoE2 in the presence of different concentrations of GuHCl. Under non-denaturing conditions, the deconvolution of the curve reveals the presence of three species as is the case for the two other isoforms. For the isoforms r-apoE2 and r-apoE4, the majority of the protein eluted in the first peak with an R_s of 6.6 nm, and corresponded to tetramer of apoE based upon the similar dimension of the plasma apoE3 tetramer [3]. The elution volumes of the second and third components suggested that they were dimer and monomer. The state of association of the isoforms was confirmed by analytical ultracentrifugation as shown in our preceding paper [1]. Under native conditions the r-apoE3 elution profile differed somewhat from that of the r-apoE2 and r-apoE4 in that, the proportion of tetramer to monomer was close to 40%, lower than the 65% observed with r-apoE2

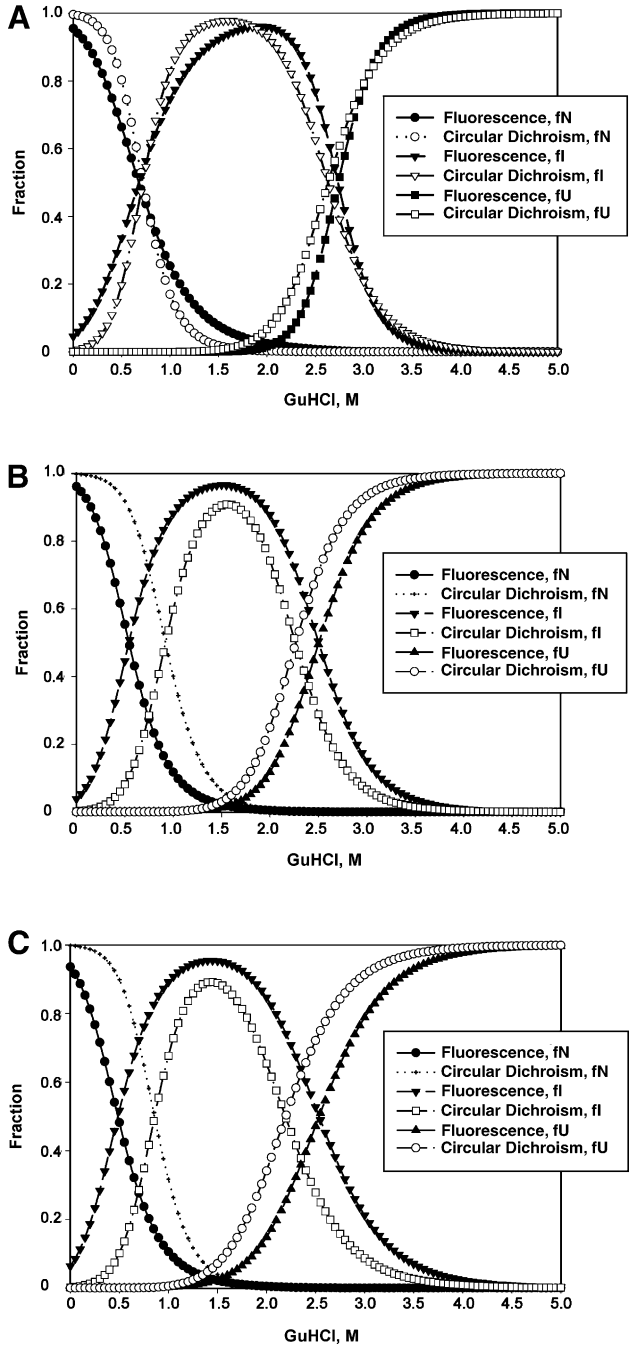

Fig. 8. Fraction of the fully folded, fully unfolded and partially unfolded states of the three recombinant apoE isoforms during denaturation with guanidine hydrochloride followed by circular dichroism and fluorescence. (A), r-apoE2; (B), r-apoE3; (C), r-apoE4.

and r-apoE4. This suggests that apoE3 is less associated than the two other isoforms [1]. The denaturation consisted of two phases for each isoform. The first phase, between 0 and 1.25 M GuHCl, corresponded to the denaturation of the CT-domain as based upon the fluorescence and circular dichroism and at the same time to the dissociation of the oligomer into monomer (Fig. 7A). The proportion of monomer, which represented only 10% of the total species present initially, increased to 100% at 1.25 M GuHCl. Between 1.25 and 4 M GuHCl, the monomer, with an unfolded CT-domain and with a folded NT-domain, had an R_s of 4 nm, while the completely unfolded monomer had an R_s of 6.6 nm.

The volume changes during the unfolding of the proteins were expressed by plotting the coefficients of

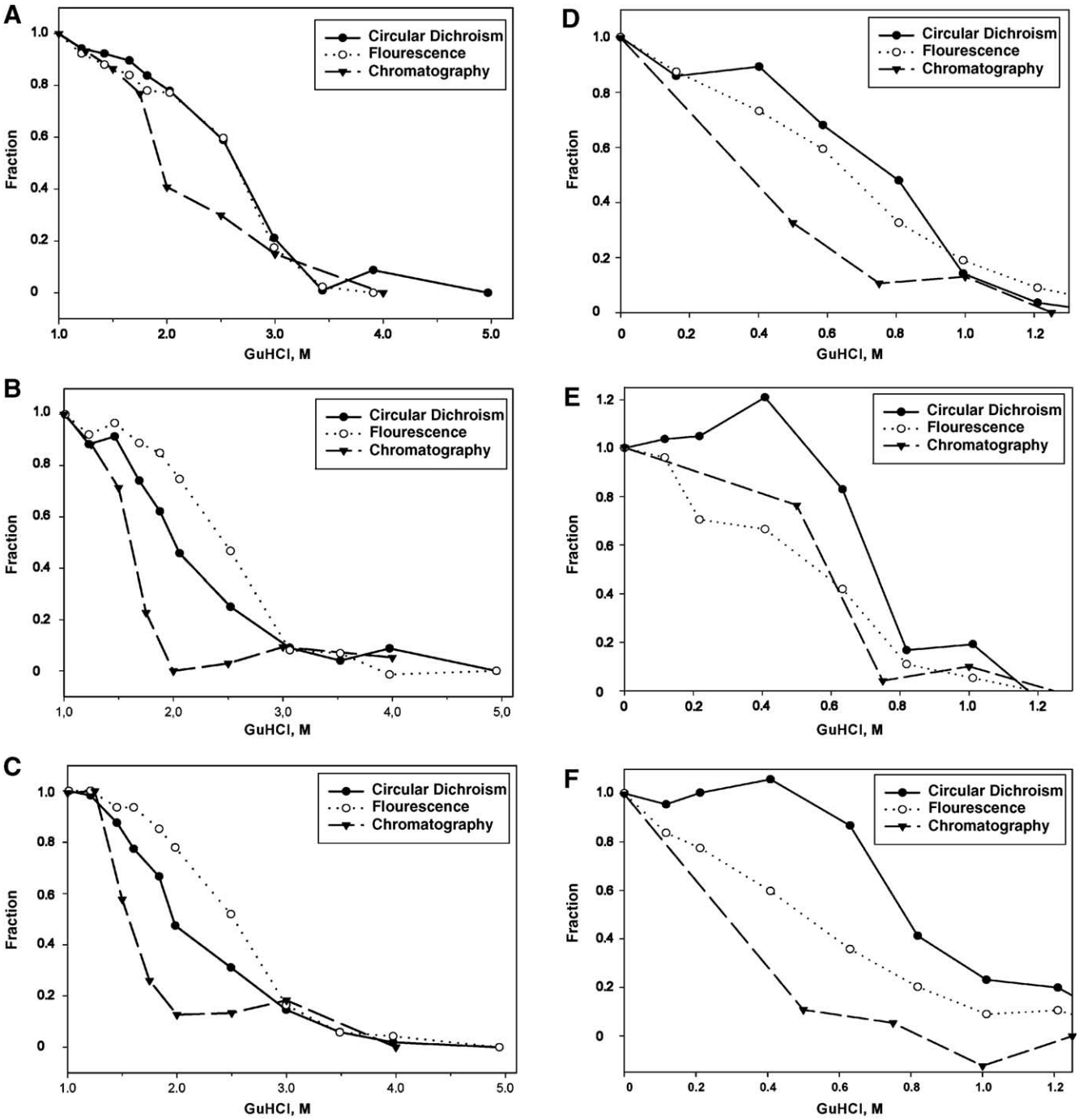

Fig. 9. Global unfolding analysis of the amino- (A–C) and carboxyl- (D–F) terminal domains of the three recombinant apoE isoforms for guanidine hydrochloride denaturation. The denaturation process was followed by three different techniques, fluorescence, circular dichroism and size-exclusion chromatography. (A,D), r-apoE2; (B,E), r-apoE3; (C,F), r-apoE4.

partition, K_D, as a function of the GuHCl concentration (Fig. 7B). The three isoforms differed in that the r-apoE4 unfolding occurred at the lowest concentrations of GuHCl whereas r-apoE2 required the largest amounts of GuHCl. This order of stability toward denaturation with GuHCl was the same as that obtained by circular dichroism and fluorescence.

3.2.4. Intermediates during unfolding

The unfolding of all three isoforms consists of at least two transitions with an intermediate composed of an unfolded CT-domain and a folded NT-domain. Determination of the values of K_{ni}, K_{iu} and K_{nu} from the three-state analysis permits the calculation of the fraction of the fully folded, fully unfolded and intermediate states (Fig. 8). Based upon these calculations, the partially folded intermediate predominates over an extended range of concentrations of GuHCl (about 1 to 2.2 M GuHCl). This is the case for all three isoforms. For each isoform the changes as followed by fluorescence precede those as followed by circular dichroism for the unfolding of the CT-domain (0–1 M GuHCl), this order is reversed for the NT-domain (2.5–4 M GuHCl). Further, these differences are more marked for r-apoE3 and r-apoE4 as opposed to r-apoE2. Considering the denaturation of the NT-domain, as assessed by the three techniques, the loss of structure of each isoform was non-coincidental (Fig. 9 A–C). For all isoforms, as assessed by size-exclusion chromatography, a specific increase in the size of the molecule was observed to occur first, and then changes in the secondary structure were observed as evaluated by circular dichroism. The denaturation curve obtained by fluorescence emission was shifted to even higher GuHCl concentrations. For apoE2, the denaturation curves obtained by far UV CD and fluorescence coincided, in contrast with those of apoE3 and apoE4, which did not. Finally, the fact that a three-state analysis gives a better fit of the experimental data than a two-state analysis suggests the presence of intermediates in the denaturation of the NT-domain.

Considering the dissociation of oligomers and the denaturation of the CT-domain, a similar global analysis was also performed for the first transition occurring between 0 and 1.2 M GuHCl (Fig. 9 D–F). In this case, for each isoform, in contrast to the NT-domain, non-coincident changes in size and fluorescence precede the loss of secondary structure reflected by circular dichroism. This suggests that the CT-domain dissociates to a large extent before unfolding.

4. Discussion

The present study provides novel information concerning three aspects of apolipoprotein E structure: (1) the relative stabilities of the three major recombinant human apoE isoforms; (2) the presence of intermediates during the denaturation of the isoforms; and (3) the similarities and the differences in the characteristics, toward denaturation, of the isolated domains as compared to the intact isoforms. We further assessed the usefulness of the recombinant isoforms as models for the intact proteins.

4.1. Thermal denaturation

Several results indicate that the recombinant isoforms, which have a 43 residue amino-terminal extension, are useful models for the plasma proteins. The very similar near and far UV CD spectra attest to the overall similarities in the tertiary and secondary structures of the proteins. The recombinant isoforms, similarly to plasma apoE3, are composed of two structural domains and have similar structural properties as shown by limited proteolysis in the preceding paper [1], chemical and thermal denaturation (this paper). However, the r-apoE3 is less stable than the plasma protein. The differences in the stability between the recombinant and the plasma apoE3 could result from the presence of the 43 residue amino-terminal extension in the recombinant protein.

In the far UV CD region, the presence of two distinct transitions in the denaturation curve of r-apoE2 reveals an unfolding process distinct from that of r-apoE3 and r-apoE4, the curves of which apparently exhibit only one transition. The greater T_m(app) and ΔH(app) values for r-apoE2 determined from the major transition of the far UV CD experiments, as well as the higher T_m(app) value obtained from the near UV CD experiments, suggest an increased resistance of r-apoE2 to thermal unfolding as compared to r-apoE3 and to r-apoE4, which has the lowest thermal stability. That coincides with the data of Morrow et al. [24] on the high-temperature unfolding of three isoforms; however, these authors did not observe two transitions in the denaturation curve of r-apoE2. This order of stability is the same as that found with the chemical denaturation with GuHCl as assessed by the three methods and coincides with the chemical denaturation data of Morrow et al. [24]. The differences in the thermal stabilities among the isoforms could be due to intramolecular bonds that stabilize the proteins, in part due to differing interactions between the NT- and CT-domains in the isoforms. The first transition of the thermal denaturation of tetrameric r-apoE2 could be due to the dissociation of oligomers, analogous to the thermal denaturation of apoC-I [30], followed by the unfolding of the monomer. A non-cooperative dissociation of oligomers could occur in r-apoE3 and r-apoE4, in which case the first transition would be less apparent. However, this explanation can not be proposed for the first transition observed with the recombinant NT-domain, which is monomeric. In that case, the two transitions may reflect a complex process of denaturation. Moreover, one [24] or two [31] transitions at the thermal unfolding of the NT-domains of the three isoforms have been observed.

Another difference in the thermal unfolding of the isoforms is the simultaneous unfolding of the secondary (major transition) and tertiary structures of r-apoE2, as opposed to the sequential denaturation of r-apoE3 and r-apoE4 (tertiary structure first then the secondary structure). Following heating to 37 °C, the secondary structure was largely intact as compared to that of 15 °C for r-apoE2 (83%), r-apoE3 (80%), r-apoE4 (77%), and p-apoE3 (82%). The tertiary structures of r-apoE3, r-apoE4 and p-apoE3 are, however, clearly altered at 37 °C as compared to 15 °C. This suggests that, under physiological conditions, plasma and recombinant apoE3 and r-apoE4 have well-defined secondary structures but altered tertiary structures. A similar suggestion has been made by others [31]. In the cases of apoA-I [27] and apoA-II [29], compact molten globular states have been proposed to exist at physiological temperatures. Thermal denaturation of apoA-II showed a well-defined isochromatic point during heat-induced unfolding whereas there were non-coincident secondary structural changes in the course of its cold denaturation [29]. In contrast, apoA-I displays a non-two-state transition during thermal unfolding as shown by both far UV CD [27] and differential scanning calorimetry (DSC) [28]. For human plasma apoE3, the far UV CD spectra recorded at different temperatures show a single isochromatic point at 202.5 nm suggesting a two-state unfolding. Nevertheless, the non-coincident changes in the secondary and tertiary structures suggest that the unfolding of apoE may be more complex than a two-state process. However, Acharya et al. [31] were unable to detect cooperative changes in the tertiary structure of either full-length apoE or the NT- or CT-domains at thermal unfolding by monitoring tryptophan fluorescence. In contrast to the sequential alteration of the tertiary structure followed by the loss of α-helical structure for plasma and r-apoE3 and r-apoE4, there is no change in the tertiary structure between 15 °C and physiological temperature for the isolated domains.

The loss of the secondary structure upon heating of the three recombinant isoforms of apoE and the plasma apoE3 is irreversible. In contrast, the thermal denaturation of the secondary structure of apoA-II [29] and apoC-I (from 22 to 80 °C) [30] was reversible while only partial recovery of far UV CD and DSC curves occurred after re-heating of apoA-I [28]. It is remarkable that the denaturation of the secondary structure of each individual isolated domain of apoE is also reversible. The reversibility of the thermal denaturation of the NT-domains of three isoforms, as assessed by DSC, has been observed also by Acharya et al. [31]. This suggests that the presence of the two domains in the intact protein may complicate the renaturation and that interactions between the two domains might occur. This suggestion coincides, firstly, with the data of Dong and Weisgraber [19] on the specific Arg61–Glu255 interaction in apoE4, secondly, with the higher Van't Hoff enthalpy of the intact protein in far UV region as compared to those of each domain individually and, finally, with isoform-specific binding of apoE to β-amyloid, which occurs via the CT-domain [17], the sequence of which is identical for the isoforms. However, the sums of the near UV spectra of the NT-domain and the CT-domain give a spectrum almost identical to the intact protein (not shown) and suggest that, even if domain interactions (besides the specific interaction in apoE4) occur, the overall tertiary structures of the two domains in the intact protein are similar to those exhibited by the domains independently in solution. Non-specific interdomain interactions, most evident in r-apoE2 and r-apoE3, were also suggested by Acharya et al. [31].

4.2. Chemical denaturation

Far UV circular dichroism showed that, in the absence of GuHCl, the recombinant apoE isoforms contained a large α-helical content, as has been described for human plasma apoE [25,48] and three recombinant isoforms [24]. The denaturation results of the present and other [24] studies show that the three recombinant isoforms are organized into two structural domains as is the case for human plasma apoE3 [25]. The normalized denaturation curves obtained from the variations of the wavelength of the fluorescence maxima λ_{max} clearly showed two transitions in accordance with our previous data on human plasma fluorescein-labelled apoE [4]. On the other hand, Jonas et al. observed a single transition [49]. The two transitions that we observed in the denaturation of the recombinant human apoE isoforms by spectroscopic techniques were also apparent by size-exclusion chromatography. The calculation of the apparent free energies of denaturation for each of the transitions of each of the apoE isoforms showed that r-apoE4 had the lowest global $\Delta G_{n,u}$, largely due to the smaller value of the $\Delta G_{i,u}$ of its NT-domain. On the other hand, r-apoE2 was the most stable isoform with a particularly high $\Delta G_{i,u}$ for its NT-domain.

4.3. Presence of intermediates

In addition to a clearly defined intermediate characterized by an unfolded carboxyl-terminal domain and a folded amino-terminal domain, the unfolding of both the NT- and CT-domains of the recombinant apoE isoforms may be more complex than simple two-state transitions. This conclusion is based upon the results that show that the losses of secondary and tertiary structures, as determined by three different techniques, do not coincide. This particular behavior is not related to the rate of protein diffusion in the chromatographic column [50] or to the different interaction of native or unfolded proteins with Superose 12 column.

For the unfolding of the CT-domain the changes in the tertiary structure precede the changes in the secondary structure. The presence of intermediate dimer during the chemical unfolding of the recombinant CT-domain that

initially existed as tetramer (dimer of dimer) in the native state has been observed by Choy et al. [33]. Morrow et al. [24] did not observe any intermediate upon chemical or thermal unfolding of the CT-domain as assessed by far UV CD; but, two transitions in the DSC curve of the CT-domain were clearly evident [31].

In contrast, for the NT-domain, there is first an increase in the size of the molecules after which there is a loss of the secondary structure which is then followed by alteration of the tertiary structure surrounding the three tryptophan residues (24, 34 and 38) at the extremity of the first α-helix of the four-helix bundle. Thus, although the size of the molecule was increasing, the environment of the first α-helix within the NT-domain apparently did not change. This could reflect a conformational change similar to that which has been proposed to occur upon the association of apoE with lipids [51]. This change consists of opening of the tetra-helical bundle without inducing a major disruption of the α-helical structure, however, the two pairs of helices (1,2 and 3,4) are separated in space. A similar conformational change was also proposed for apolipophorin III [52]. This type of opened structure for apoE might also be present during the denaturation process. Other authors have suggested the presence of a folding intermediate in the NT-domain of apoE, most prominently in apoE4 [24,31,32]. At lower GuHCl concentrations, the four-helix bundle could open without an accompanying change in the secondary structure and without inducing a change in the interactions of the first helix with the second helix. The denaturation of r-apoE3 and r-apoE4 assessed by circular dichroism occurs at lower GuHCl concentrations compared to that by fluorescence, in agreement with the data of Morrow et al. on the NT-domains of r-apoE3 and r-apoE4 [24]. The first α-helix thus seems more stable than the rest of the bundle. The higher stability of helix 1 has been also suggested by Acharya et al. [31]. This shift was not observed for the r-apoE2, for which the secondary structure appeared more stable than those of r-apoE3 and r-apoE4, probably, due to specific interactions within r-apoE2.

4.4. Multiple-state denaturation of apoE: a more rigorous evaluation

A three-state model for the denaturation of apoE may be an oversimplification. Two (I_1 and I_2) or more intermediate kinetic and equilibrium states in protein folding have been described [53]. A minimal scheme, as applied to apoE, could be: $N \leftrightarrow I_1 \leftrightarrow I_2 \leftrightarrow U$. An isoform dependent population of the intermediates may be then suggested as follows: $I_1 < I_2$ for r-apoE2, $I_1 \approx I_2$ for r-apoE3 and $I_1 > I_2$ for r-apoE4. This distribution follows from: (1) the more "irreversible" nature of the thermal denaturation of r-apoE4; (2) the increased cooperativity of the temperature-induced transitions of r-apoE2 as assessed by far UV CD and r-apoE4 as assessed by near UV CD, respectively; (3) the increase of the α parameter in GuHCl denaturation as r-apoE4 < r-apoE3 < r-apoE2; (4) the lowest and the highest values of $\Delta G_{n,i}$ for r-apoE4 calculated from fluorescence and circular dichroism measurements; (5) the highest $\Delta G_{i,u}$ value for GuHCl denaturation of r-apoE2 as assessed by fluorescence. Tertiary structure contributes preferentially to the I_1 state as assessed by fluorescence and the secondary structure to the I_2 state as assessed by far UV CD.

How many transitions in the structure of the three apoE isoforms may be inferred from two kinds of perturbations as assessed by different methods?

By size-exclusion chromatography, at least three GuHCl-induced transitions are visible. The first transition (0–0.5 M) may correspond to dissociation of the apoE, self-associated as tetramer via CT-domain, to an oligomer* (I_1-state) with smaller dimensions, e.g. a dimer. The I_1 and N states may correspond to the populations of the "open" and "closed" conformers of self-associated plasma apoE at 4 °C and after heating, respectively [5]). The second transition (0.5–1.25 M) may correspond to the parallel dissociation and denaturation of this oligomer* to a monomer (I_2-state) with a contribution of both processes for r-apoE3, whereas the oligomer* is the more populated for r-apoE4. The third transition (1.25–3 M) with some heterogeneity for r-apoE2 may correspond to denaturation of the monomer to the fully unfolded state (U-state). (The small, if any, amplitude of the first transition as assessed by fluorescence and CD measurements for r-apoE2, probably, reflects the higher degree of self-association of this isoform as compared to two others [1], the dimer of r-apoE2 and the monomers of r-apoE3 and r-apoE4 may be the basic units of apoE structure).

By fluorescence, three GuHCl-induced transitions are apparent within the ranges of concentration of 0–0.3, 0.3–0.7 and 0.7–3.0 M GuHCl.

By far UV CD, up to four GuHCl-induced transitions are visible: the first one (0–0.3 M) may correspond to the formation of a superhelical oligomer* structure with its subsequent denaturation to a monomer (I_2-state) within the concentration range 0.3–1.0 M GuHCl; the third transition (1.0–1.7 M), most prominent for r-apoE4, may correspond to the denaturation to a monomer* with altered constraints in tertiary structure within the NT-domain (I_3-state); the last transition (1.7– 3.0 M), most prominent for r-apoE2, may correspond to the denaturation of the rest of the molecule to a fully denatured monomer. By thermal denaturation, one (20–60 °C, r-apoE3 and r-apoE4) or two (20–30 °C, 40–60 °C, r-apoE2) transitions are visible. The two transitions observed upon thermal denaturation of the isolated CT- and NT-domains (Fig. 2) may correspond to the dissociation of self-associated structures and to subsequent unfolding of individual secondary structures.

By near UV CD, despite low signal-to-noise ratio, several zones of the stability of tertiary structure may be identified: the region of maximal stability around 20 °C, the decrease at low (<20 °C) and elevated temperatures (20–35 °C, r-apoE3

and r-apoE4; 20–40 °C, r-apoE2), high-temperature unfolding (30–45 °C, r-apoE3 and r-apoE4; 40–60 °C, r-apoE2) and an aggregation zone (>50 °C, r-apoE3 and r-apoE4; >60 °C, r-apoE2).

Due to the non-coincidence of the transition zones, four transitions between five equilibrium states that included three intermediate states may be postulated for apoE in solution according to the scheme below.

Oligomer (N) ↔ oligomer* (I_1) ↔ monomer (I_2) ↔ monomer*(I_3) ↔ unfolded monomer (U).

Gel-fitration (GuHCl)	<=>	<=>	<==========>
Fluorescence (GuHCl)	<=>	<=>	<==========>
FarUV-CD (GuHCl)	<==========>	<=>	<=>
FarUV-CD (T)	<==========>	<==========>	
NearUV- CD (T)	<==========>	<==========>	

4.5. Conclusion

The results of the present study have shown that there are isoform-specific differences in the stabilities of the intact proteins and their domains as revealed by global denaturation analyses. The r-apoE4 isoform is the least stable whereas the r-apoE2 isoform is the most stable. The differences in stability of the isoforms are related in part to their different self-association states. Further, the global analysis suggests that the unfolding of both the amino-terminal and carboxyl-terminal domains are more complicated than two-state transitions which had previously been assumed and may be related to conformational changes which occur upon binding to lipids and to dissociation of a tetrameric structure. Different domain interactions in the three apoE isoforms may be at the origin of the differences in the interactions of the isoforms with tau, β-amyloid and the LDL receptor.

Acknowledgements

This work was supported in part by the Centre National de la Recherche Scientifique (C.N.R.S.), the Institut National de la Santé et de la Recherche Médicale (I.N.S.E.R.M.), by the Caisse Nationale de l'Assurance Maladie des Travailleurs Salariés (C.N.A.M.T.S.), the Ministère de l'Enseignement Supérieur et de la Recherche, the Fondation Pour la Recherche Médicale and the European Economic Community (contract MAT1-CT94046). A.D.D. thanks the Russian Foundation for Basic Research for financial support, grant 04-04-48165.

References

[1] A. Barbier, V. Clement-Collin, A.D. Dergunov, A. Visvikis, G. Siest, L.P. Aggerbeck, The structure of three recombinant apolipoprotein E isoforms in solution: 1. Tertiary and quaternary structure, Biophys. Chemist. 119 (2005) 174–185. doi:10.1016/j.bpc.2005.07.010.

[2] C. Wilson, M.R. Wardell, K.H. Weisgraber, R.W. Mahley, D.A. Agard, Three-dimensional structure of the LDL receptor-binding domain of human apolipoprotein E, Science 252 (1991) 1817–1822.

[3] L.P. Aggerbeck, J.R. Wetterau, K.H. Weisgraber, C.S. Wu, F.T. Lindgren, Human apolipoprotein E3 in aqueous solution: II. Properties of the amino- and carboxyl-terminal domains, J. Biol. Chem. 263 (1988) 6249–6258.

[4] A.D. Dergunov, V.V. Shuvaev, E.V. Yanushevskaja, Quaternary structure of apolipoprotein E in solution: fluorimetric, chromatographic and immunochemical studies, Biol. Chem. Hoppe-Seyler 373 (1992) 323–331.

[5] A.D. Dergunov, Y.Y. Vorotnikova, S. Visvikis, G. Siest, Homo- and hetero-complexes of exchangeable apolipoproteins in solution and in lipid-bound form, Spectrochim. Acta, Part A 59 (2003) 1127–1137.

[6] H. Saito, P. Dhanasekaran, F. Baldwin, K.H. Weisgraber, S. Lund-Katz, M.C. Phillips, Lipid binding-induced conformational change in human apolipoprotein E. Evidence for two lipid-bound states on spherical particles, J. Biol. Chem. 276 (2001) 40949–40954.

[7] H. Saito, P. Dhanasekaran, D. Nguyen, P. Holvoet, S. Lund-Katz, M.C. Phillips, Domain structure and lipid interaction in human apolipoproteins A-I and E, a general model, J. Biol. Chem. 278 (2003) 23227–23232.

[8] V. Clement-Collin, A. Leroy, C. Monteilhet, L.P. Aggerbeck, Mimicking lipid-binding-induced conformational changes in the human apolipoprotein E N-terminal receptor binding domain effects of low pH and propanol, Eur. J. Biochem. 264 (1999) 358–368.

[9] C.A. Fisher, V. Narayanaswami, R.O. Ryan, The lipid-associated conformation of the low density lipoprotein receptor binding domain of human apolipoprotein E, J. Biol. Chem. 275 (2000) 33601–33606.

[10] B. Lu, J.A. Morrow, K.H. Weisgraber, Conformational reorganization of the four-helix bundle of human apolipoprotein E in binding to phospholipid, J. Biol. Chem. 275 (2000) 20775–20781.

[11] V. Raussens, C.A. Fisher, E. Goormaghtigh, R.O. Ryan, J.M. Ryusschaert, The low density lipoprotein receptor active conformation of apolipoprotein E. Helix organization in N-terminal domain-phospholipid disc particles, J. Biol. Chem. 273 (1998) 25825–25830.

[12] V. Raussens, C.M. Slupsky, R.O. Ryan, B.D. Sykes, NMR structure and dynamics of a receptor-active apolipoprotein E peptide, J. Biol. Chem. 277 (2002) 29172–29180.

[13] V. Raussens, C.M. Slupsky, B.D. Sykes, R.O. Ryan, Lipid-bound structure of an apolipoprotein E-derived peptide, J. Biol. Chem. 278 (2003) 25998–26006.

[14] P.M. Weers, V. Narayanaswami, R.O. Ryan, Modulation of the lipid binding properties of the N-terminal domain of human apolipoprotein E3, Eur. J. Biochem. 268 (2001) 3728–3735.

[15] S. Lund-Katz, S. Wehrli, M. Zaiou, Y. Newhouse, K.H. Weisgraber, M.C. Phillips, Effects of polymorphism on the microenvironment of the LDL receptor-binding region of human apoE, J. Lipid Res. 42 (2001) 894–901.

[16] M. Perugini, P. Schuck, G.J. Howlett, Self-association of human apolipoprotein E3 and E4 in the presence and absence of phospholipid, J. Biol. Chem. 275 (2000) 36758–36765.

[17] T. Pillot, M. Goethals, J. Najib, C. Labeur, L. Lins, J. Chambaz, R. Brasseur, J. Vandekerckhove, M. Rosseneu, Beta-amyloid peptide interacts specifically with the carboxy-terminal domain of human apolipoprotein E: relevance to Alzheimer's disease, J. Neurochem. 72 (1999) 230–237.
[18] L.M. Dong, C. Wilson, M.R. Wardell, T. Simmons, R.W. Mahley, K.H. Weisgraber, D.A. Agard, Human apolipoprotein E. Role of arginine 61 in mediating the lipoprotein preferences of the E3 and E4 isoforms, J. Biol. Chem. 269 (1994) 22358–22365.
[19] L.M. Dong, K.H. Weisgraber, Human apolipoprotein E4 domain interaction. Arginine 61 and glutamic acid 255 interact to direct the preference for very low density lipoproteins, J. Biol. Chem. 271 (1996) 19053–19057.
[20] M.A. Perugini, P. Schuck, G.J. Howlett, Differences in the binding capacity of human apolipoprotein E3 and E4 to size-fractionated lipid emulsions, Eur. J. Biochem. 269 (2002) 5939–5949.
[21] H. Saito, P. Dhanasekaran, F. Baldwin, K.H. Weisgraber, M.C. Phillips, S. Lund-Katz, Effects of polymorphism on the lipid interaction of human apolipoprotein E, J. Biol. Chem. 278 (2003) 40723–40729.
[22] M.L. Segall, P. Dhanasekaran, F. Baldwin, G.M. Anantharamaiah, K.H. Weisgraber, M.C. Phillips, S. Lund-Katz, Influence of apoE domain structure and polymorphism on the kinetics of phospholipid vesicle solubilization, J. Lipid Res. 43 (2002) 1688–1700.
[23] L.M. Dong, T.L. Innerarity, K.S. Arnold, Y.M. Newhouse, K.H. Weisgraber, The carboxyl terminus in apolipoprotein E2 and the seven amino acid repeat in apolipoprotein E-Leiden: role in receptor-binding activity, J. Lipid Res. 39 (1998) 1173–1180.
[24] J.A. Morrow, M.L. Segall, S. Lund-Katz, M.C. Phillips, M. Knapp, B. Rupp, K.H. Weisgraber, Differences in stability among the human apolipoprotein E isoforms determined by the amino-terminal domain, Biochemistry 39 (2000) 11657–11666.
[25] J.R. Wetterau, L.P. Aggerbeck, S.C. Rall Jr., K.H. Weisgraber, Human apolipoprotein E3 in aqueous solution: I. Evidence for two structural domains, J. Biol. Chem. 263 (1988) 6240–6248.
[26] Y. Fang, O. Gursky, D. Atkinson, Structural studies of N- and C-terminally truncated human apolipoprotein A-I, Biochemistry 42 (2003) 6881–6890.
[27] O. Gursky, D. Atkinson, Thermal unfolding of human high-density apolipoprotein A-1: implications for a lipid-free molten globular state, Proc. Natl. Acad. Sci. U. S. A. 93 (1996) 2991–2995.
[28] M. Suurkuusk, D. Hallen, Denaturation of apolipoprotein A-I and the monomer form of apolipoprotein A-I (Milano), Eur. J. Biochem. 265 (1999) 346–352.
[29] O. Gursky, D. Atkinson, High- and low-temperature unfolding of human high-density apolipoprotein A-2, Protein Sci. 5 (1996) 1874–1882.
[30] O. Gursky, D. Atkinson, Thermodynamic analysis of human plasma apolipoprotein C-1: high-temperature unfolding and low-temperature oligomer dissociation, Biochemistry 37 (1998) 1283–1291.
[31] P. Acharya, M.L. Segall, M. Zaiou, J. Morrow, K.H. Weisgraber, M.C. Phillips, S. Lund-Katz, J. Snow, Comparison of the stabilities and unfolding pathways of human apolipoprotein E isoforms by differential scanning calorimetry and circular dichroism, Biochim. Biophys. Acta 1584 (2002) 9–19.
[32] J.A. Morrow, D.M. Hatters, B. Lu, P. Hochtl, K.A. Oberg, B. Rupp, K.H. Weisgraber, Apolipoprotein E4 forms a molten globule. A potential basis for its association with disease, J. Biol. Chem. 277 (2002) 50380–50385.
[33] N. Choy, V. Raussens, V. Narayanaswami, Inter-molecular coiled-coil formation in human apolipoprotein E C-terminal domain, J. Mol. Biol. 334 (2003) 527–539.
[34] G. Wang, G.K. Pierens, W.D. Treleaven, J.T. Sparrow, R.J. Cushley, Conformations of human apolipoprotein E(263–286) and E(267–289) in aqueous solutions of sodium dodecyl sulfate by CD and 1H NMR, Biochemistry 35 (1996) 10358–10366.
[35] T. Pillot, A. Barbier, A. Visvikis, K. Lozac'h, M. Rosseneu, J. Vandekerckhove, G. Siest, Single-step purification of two functional human apolipoprotein E variants hyperexpressed in *Escherichia coli*, Protein Expr. Purif. 7 (1996) 407–414.
[36] A. Barbier, A. Visvikis, F. Mathieu, L. Diez, L.M. Havekes, G. Siest, Characterization of three human apolipoprotein E isoforms (E2, E3 and E4) expressed in *Escherichia coli*, Eur. J. Clin. Chem. Clin. Biochem. 35 (1997) 581–589.
[37] C. Monteilhet, N. Lachacinski, L.P. Aggerbeck, Cytoplasmic and periplasmic production of human apolipoprotein E in *Escherichia coli* using natural and bacterial signal peptides, Gene 125 (1993) 223–228.
[38] K.H. Weisgraber, S.C. Rall Jr., R.W. Mahley, Human E apoprotein heterogeneity. Cysteine–arginine interchanges in the amino acid sequence of the apo-E isoforms, J. Biol. Chem. 256 (1981) 9077–9083.
[39] P. Pajot, Fluorescence of proteins in 6-M guanidine hydrochloride. A method for the quantitative determination of tryptophan, Eur. J. Biochem. 63 (1976) 263–269.
[40] H.J. Pownall, J.B. Massey, Spectroscopic studies of lipoproteins, Methods Enzymol. 128 (1986) 515–518.
[41] Y.H. Chen, J.T. Yang, H.M. Martinez, Determination of the secondary structures of proteins by circular dichroism and optical rotatory dispersion, Biochemistry 11 (1972) 4120–4131.
[42] C.A. Royer, C.J. Mann, C.R. Matthews, Resolution of the fluorescence equilibrium unfolding profile of trp aporepressor using single tryptophan mutants, Protein Sci. 2 (1993) 1844–1852.
[43] M. Le Maire, L.P. Aggerbeck, C. Monteilhet, J.P. Andersen, J.V. Moller, The use of high-performance liquid chromatography for the determination of size and molecular weight of proteins: a caution and a list of membrane proteins suitable as standards, Anal. Biochem. 154 (1986) 525–535.
[44] V.N. Uversky, Use of fast protein size-exclusion liquid chromatography to study the unfolding of proteins which denature through the molten globule, Biochemistry 32 (1993) 13288–13298.
[45] C. Tanford, Protein denaturation, Adv. Protein Chem. 23 (1968) 121–282.
[46] S.W. Tendian, D.G. Myszka, R.W. Sweet, I.M. Chaiken, C.G. Brouillette, Interdomain communication of T-cell CD4 studied by absorbance and fluorescence difference spectroscopy measurements of urea-induced unfolding, Biochemistry 34 (1995) 6464–6474.
[47] C.R. Matthews, M.M. Crisanti, Urea-induced unfolding of the alpha subunit of tryptophan synthase: evidence for a multistate process, Biochemistry 20 (1981) 784–792.
[48] S. Yokoyama, Y. Kawai, S. Tajima, A. Yamamoto, Behavior of human apolipoprotein E in aqueous solutions and at interfaces, J. Biol. Chem. 260 (1985) 16375–16382.
[49] A. Jonas, A. Steinmetz, L. Churgay, The number of amphipathic alpha-helical segments of apolipoproteins A-I, E, and A-IV determines the size and functional properties of their reconstituted lipoprotein particles, J. Biol. Chem. 268 (1993) 1596–1602.
[50] V.N. Uversky, O.B. Ptitsyn, Further evidence on the equilibrium "pre-molten globule state": four-state guanidinium chloride-induced unfolding of carbonic anhydrase B at low temperature, J. Mol. Biol. 255 (1996) 215–228.
[51] K.H. Weisgraber, Apolipoprotein E: structure–function relationships, Adv. Protein Chem. 45 (1994) 249–302.
[52] D.R. Breiter, M.R. Kanost, M.M. Benning, G. Wesenberg, J.H. Law, M.A. Wells, I. Rayment, H.M. Holden, Molecular structure of an apolipoprotein determined at 2.5-A resolution, Biochemistry 30 (1991) 603–608.
[53] H.C. Hung, Y.H. Chen, G.Y. Liu, H.J. Lee, G.G. Chang, Equilibrium protein folding–unfolding process involving multiple intermediates, Bull. Math. Biol. 65 (2003) 553–570.